TRR
JOURNAL OF THE TRANSPORTATION RESEARCH BOARD

Research Article

Transportation Research Record
1–9

DOI: 10.1177/0361198119852337
journals.sagepub.com/home/trr
SAGE

Impact of Time-Varying Passenger Loading on Conventional and Electrified Transit Bus Energy Consumption

Luying Liu[1], Andrew Kotz[2], Aditya Salapaka[1], Eric Miller[2], and William F. Northrop[1]

Abstract

Transit bus passenger loading changes significantly over the course of a workday. Therefore, time-varying vehicle mass as a result of passenger load becomes an important factor in instantaneous energy consumption. Battery-powered electric transit buses have restricted range and longer "fueling" time compared with conventional diesel-powered buses; thus, it is critical to know how much energy they require. Our previous work has shown that instantaneous transit bus mass can be obtained by measuring the pressure in the vehicle's airbag suspension system. This paper leverages this novel technique to determine the impact of time-varying mass on energy consumption. Sixty-five days of velocity and mass data were collected from in-use transit buses operating on routes in the Twin Cities, MN metropolitan area. The simulation tool Future Automotive Systems Technology Simulator was modified to allow both velocity and mass as time-dependent inputs. This tool was then used to model an electrified and conventional bus on the same routes and determine the energy use of each bus. Results showed that the kinetic intensity varied from 0.27 to 4.69 mi^{-1} and passenger loading ranged from 2 to 21 passengers. Simulation results showed that energy consumption for both buses increased with increasing vehicle mass. The simulation also indicated that passenger loading has a greater impact on energy consumption for conventional buses than for electric buses owing to the electric bus's ability to recapture energy. This work shows that measuring and analyzing real-time passenger loading is advantageous for determining the energy used by electric and conventional diesel buses.

Fuel cost is the second largest expense for transit bus operators following driver salary. According to data from 2006, fuel costs contributed to 45% of the total service costs for conventional diesel-powered buses (*1*). The same source showed that there were 976,000 in-service buses in 2016, 259% more than in 1960. At an assumed fuel economy of 7.3 mpg, 2.226 billion gallons of total fuel was consumed that year, equating to an average of 228 gal per vehicle (*2*).

High yearly fuel consumption has motivated the implementation of hybrid-electric systems over the past two decades. According to American Public Transportation Association statistics, 16.9% of public transit buses were hybrid-electric, using a diesel engine combined with an electric traction motor and battery to reclaim energy through regenerative braking. The share of hybrid-electric buses increased from 1% in 2005 to nearly 17% in 2015. Efficiency gains from hybridizing are not without costs; they require transit authorities to maintain both electric and conventional vehicle components including batteries and diesel engines with associated after treatment hardware. Hardware and maintenance costs reduce the lifetime financial benefit of hybrid vehicles (*3*).

The high operating costs of hybrid-electric buses and improved battery economics have motivated a switch to full electrification of transit fleets. Simultaneously, forecasted increases in transit use are expected to result in a growth of the global market for battery electric transit buses from nearly 119,000 buses in 2016 to over 181,000 in 2026 (*4*). Implementing fully electrified buses on arterial routes enhances mobility while significantly improving energy productivity and reducing emissions.

Many in-use factors influence the energy consumption of transit buses, whether that energy is consumed as a

[1]Department of Mechanical Engineering, University of Minnesota, Minneapolis, MN
[2]National Renewable Energy Laboratory, Golden, CO

Corresponding Author:
Address correspondence to William F. Northrop: wnorthro@umn.edu

liquid fuel in conventional diesel buses (CDBs) or an electrical charge in battery electric buses (BEBs). Such factors include air conditioning use (*5*), auxiliary diesel heating (*5*), driver behavior (*6*), route type (*7*), traffic (*7*), and passenger mass. Zhang et al. showed that average bus fuel consumption increased from 19% to 33% when average speed decreased from 25 to 15 km/h in transit buses (*8*). They found that fuel consumption associated with air conditioning systems was considerable, increasing fuel use by 23% when the system was on. They also showed that hybrid buses could reduce fuel consumption between 18% and 29% for the same distance compared with CDBs. The impacts of speed and air conditioning systems were much greater in hybrids, with a 50% increase of fuel usage for average speed decreasing from 25 to 15 km/h and a 48% increase for operating air conditioning systems. Most of the aforementioned factors have been extensively studied, with the exception of passenger mass. Some have studied the influence of mass on light-duty vehicles with different powertrain configurations (*9*), but few have studied its impact on transit bus energy use. Estimating the mass of commercial vehicles is difficult because they operate over a wide range of vehicle weight. Transit buses are an exceptional case as mass varies constantly as a result of passengers boarding and alighting.

The vehicle power equation (Equation 1) illustrates the impact of vehicle mass on power consumption. In Equation 1, P is the power required, m is the total vehicle mass, a is the acceleration of the vehicle, v is the vehicle speed, c_{rr} is the vehicle coefficient of rolling resistance, g is the gravitational acceleration, θ is the road gradient angle, c_d is the drag coefficient of the vehicle, A is vehicle equivalent cross-sectional area, and ρ is air density. The first term is the acceleration term; the second accounts for rolling resistance; the third represents air drag; the fourth is road grade; and the final is for regenerative braking. Of those, the power required for acceleration, rolling resistance and road grade all increase linearly with the mass of the vehicle.

$$P = \text{mav} + c_{rr}\text{mgvcos}\theta + \frac{1}{2}c_d A\rho v^3 + \text{mgvsin}\theta \qquad (1)$$

Although it is known that transit bus mass, and therefore energy consumption through Equation 1, changes constantly during a route because of passenger boarding and alighting, most previous modeling work has considered it to be constant. Few studies have considered time-varying passenger load in bus energy consumption. In the most pertinent work, Yu et al. used second-by-second vehicle data and recorded passenger number to determine CDB mass using 50 kg as the average passenger weight (*10*). Passenger load, vehicle speed, and acceleration were divided into different segments, and bus fuel consumption was calculated under those intervals. They found that the impact of passenger load on fuel consumption rates became significant when the buses traveled at speeds over 30 km/h or accelerated faster than 0.1 m/s^2. No clear trends were shown illustrating that the passenger load had any influence on the distance-specific fuel consumption for low or high-speed periods; however, the per-passenger fuel consumption decreased with increasing passenger load.

A shortcoming of previous research is that most use average speed rather than instantaneous speed when calculating fuel consumption. Fuel consumption using average speed is less insightful because it does not capture high or low speed extremes on a route and is insensitive to acceleration rate. Furthermore, most fuel consumption research related to vehicle mass has been conducted in large Chinese cities, such as Beijing and Hong Kong (*8, 11, 12*). On account of the unusual driving conditions in the urban areas of those cities, results may not be applicable to less congested U.S. or European cities where vehicles accelerate and decelerate less frequently.

In this paper, we apply a novel bus mass detection technique to determine the impact of time-varying mass on bus energy consumption. Unlike previous studies that use a constant mass or estimate varying mass using average passenger weight, vehicle mass and speed were directly measured from in-use transit buses. The information was then used as input for a vehicle model to estimate the energy use of simulated BEBs and CDBs. One valuable use of the analysis presented here is to predict how BEB range is affected by mass changes resulting from realistic passenger loading. More closely examining the effects of varying mass on fuel consumption can help public transportation companies plan more efficient routes and timetables. The method described in this paper could be adapted to compute the fuel refill quantity in CDBs or recharging time in BEBs that use on-route fast charging. Further, understanding long-term route mass-estimates could inform future infrastructure such as in-ground wireless charging placement or distributed high draw energy storage.

Experimental Methods and Data Processing

Data Collection and Experimental Design

Most transit buses today are manufactured with air ride suspension systems to maintain the ride height and adjust suspension spring rate of buses with varying load, thereby improving passenger comfort and convenience. A mechanical auto-leveling valve is used to maintain ride height and increase or decrease spring rate by adjusting the air pressure inside the bag. The airbag pressure will increase when a passenger boards the bus and will decrease as the passenger alights.

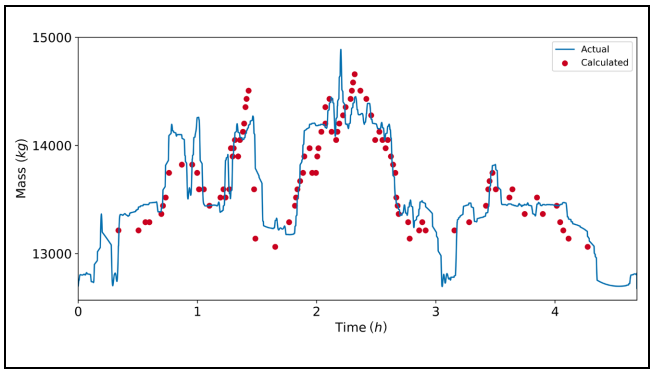

Figure 1. Actual total mass and calculated mass versus time during a route. Calculated mass assumed an average passenger mass of 76 kg.

Standard 40-ft buses, the subject of this research, have three air circuits with two connected airbags on each circuit. The three circuits are the curbside circuit referring to the rear right side or passenger pickup side of the vehicle; the street-side circuit referring to the rear driver's side; and the front circuit, which encompasses both the front driver's and passenger pickup side of the bus. Our, previous research showed that the mass of a bus is proportional to the combined pressure in the airbags. Equation 2 shows the estimated mass of the bus, m_{bus}, where P_{Front}, P_{Curb}, P_{Street} are the pressures measured in each airbag respectively, and b_{Front}, b_{Curb}, b_{Street}, K are the constants used to correlate the interaction between the different air circuits.

$$m_{\text{bus}} = b_{\text{Front}}{}^{*}P_{\text{Front}} + b_{\text{Curb}}{}^{*}P_{\text{Curb}} + b_{\text{Street}}{}^{*}P_{\text{Street}} + K \quad (2)$$

Simplifying this expression, we assume that $K = 0$ and $b_{\text{Front}} = b_{\text{Curb}} = b_{\text{Street}}$, which gives Equation 3.

$$m_{\text{bus}} = b^{*}(P_{\text{Front}} + P_{\text{Curb}} + P_{\text{Street}}) \quad (3)$$

To verify our approach, we used a manually counted passenger number and an average passenger mass of 76 kg to calculate the actual mass (*13*). Since the fuel weight of a CDB is relatively small compared with the weight of the bus (<0.5%), it is reasonable to incorporate it into the curb weight of the vehicle. The results of the mass comparison are shown in Figure 1 in which we find that the difference in actual mass and mass calculated by airbag pressures is small. The maximum difference is 649 kg, which is 5.0% of the curb weight; however, the average difference is closer to 373 kg resulting in an error of 2.9%.

Data for the study were collected from three buses operated by Metro Transit, the primary public transit provider for the Minneapolis/St. Paul Twin Cities area in the state of Minnesota. The 40-ft Gillig low-floor buses had pressure transducers obtained from Honeywell or Omega Engineering installed in each air suspension circuit. These transducers converted the pressure in each airbag to an analog electrical signal that was then digitized via an ADS1115-based Adafruit Analog-to-Digital converter and stored locally on a Raspberry Pi 3 with an SD-card. Vehicle speed information was obtained from the J1939 CAN signals, which were interpreted by an MCP2515-based SK Pang's PiCAN2 connected to the Raspberry Pi using the socket-can protocol. With vehicle mass information needed only during stop events to calculate passenger load, data was collected at 1 Hz when the bus was in motion. At lower speeds (<3 km/h) higher resolution data necessitated an increased frequency of 30 Hz for data collection. The raw data files included the time of collection, the raw values converted from the analog electrical signal and the speed of the bus. The Raspberry Pi was also equipped with a 3G wireless modem to remotely access and transfer data wirelessly when needed. Additionally, offline data retrieval was also available through easily accessible USB and Ethernet ports that are standard on the Raspberry Pi.

To estimate bus mass, the air suspension pressures were first added using Equation 3, which translates the sum of the pressures into mass. Next, the calibration factor, b in Equation 3 was found by taking the curb weight divided by the average airbag pressure when the bus was empty. After identifying the calibration factor, speed data were used to determine when the vehicle was at a stop and thus when the vehicle mass could change. If speed changed from some positive value to zero, and the zero-speed condition lasted for more than 3 s, a stop was detected. At each stop event, pressure data was recorded for the last 3 s of the stop, filtered and then averaged to determine the pressure value inputs of Equation 3. The average of the filtered mass data for each stop was used as the mass until the next stop. Data for this study were collected between November 2017 and June 2018 from three buses resulting in a total of 65 vehicle-days with vehicle route changing daily.

Drivetrain Modeling

Several different models for vehicle fuel consumption exist, but most of these require detailed data and experts with enough knowledge to run them (*14*). Future Automotive Systems Technology Simulator (FASTSim) is a model developed by the National Renewable Energy Laboratory that requires only limited data as input but provides suitable accuracy for a study of daily energy consumption (*15*). The FASTSim model was modified from a power-based calculation to a speed-/torque-based calculation to add fidelity for commercial vehicles that

frequently encounter situations in which they are power limited, like when climbing steep hills under heavy loads. Models were constructed to estimate BEB and CDB energy consumption from the collected in-use mass and speed data.

FASTSim is a backward-looking model, meaning that with knowledge of the vehicle state, it calculates the power required to achieve that state. Inputs to the model are vehicle speed, road grade, and the data sampling increment (time step). This variant of the model is comprised of numerous sub-models, each approximating a component in the physical vehicle. Each model component has a front and back location. If two components are connected, then the back of one component is equivalent to the front of the other. For example, torque, τ, is transferred from the differential to the wheel, therefore, these components are adjacent, and the model recognizes the equality shown in Equation 4.

$$\tau_{b,\,\text{wheel}} = \tau_{f,\,\text{differential}} \tag{4}$$

Individual component models take a backward step to calculate values at the back of the component from values at the front of the component. For example, the backward step to calculate wheel torque is shown in Equation 5.

$$\tau_b = F_f r_{\text{tire}} \tag{5}$$

Each component takes a backward step in the series with the model using logged data to work backward to the battery in the case of a BEB. Equation 6 shows the series of this model transition.

$$\begin{aligned}\text{Battery} \leftarrow \text{Motor} \leftarrow \text{Transmission} \leftarrow \text{Differential} \leftarrow \\ \text{Wheel} \leftarrow \text{Chassis} \leftarrow \text{Logged Data}\end{aligned} \tag{6}$$

Once all components have completed a backward step, they take a forward step to confirm that each component was able to provide adequate power to meet the drive cycle. The progression of this forward step is illustrated in Equation 7 for a BEB.

$$\begin{aligned}\text{Battery} \rightarrow \text{Motor} \rightarrow \text{Transmission} \rightarrow \text{Differential} \rightarrow \\ \text{Wheel} \rightarrow \text{Chassis} \rightarrow \text{Model Output}\end{aligned} \tag{7}$$

If the available power from the drivetrain is less than the power required to meet the drive cycle trace, the forward step of the solver will estimate the speed that the vehicle was able to reach with reduced power.

Backward Step. Beginning with the road load equation calculated from logged speed and road grade, the chassis component calculates the road load using Equation 8 (derived from Equation 1) where $\hat{v}$ is the logged vehicle speed, and v is the modeled vehicle speed from the previous time step.

$$F_{\text{road}} = \frac{m(\hat{v} - v)}{\Delta t} + \text{mgsin}(\theta) + \frac{1}{2}\rho C_d A \hat{v} v + mgC_{rr}\cos(\theta) \tag{8}$$

The road load force (Equation 8), equivalent to the force required at the front of the tire (Equation 9), and half-step vehicle speed (Equation 10) are given as inputs to the wheel component, adhering to the rule that the back location of the chassis is equivalent to the front location of the wheel.

$$F_f = F_{\text{road}} \tag{9}$$

$$v_f = \frac{1}{2}(\hat{v} + v) \tag{10}$$

The wheel model converts linear speed and force to angular speed (Equation 11) and torque (Equation 12) with knowledge of the wheel radius.

$$\omega_b = \frac{v_f}{r_{\text{tire}}} \tag{11}$$

$$\tau_b = F_f r_{\text{tire}} \tag{12}$$

Components with gears will modify the speed and torque using Equations 13 and 14 respectively and knowledge of the gear ratio.

$$\omega_b = \omega_f r_{\text{gear}} \tag{13}$$

$$\tau_b = \frac{\tau_f}{r_{\text{gear}}} \tag{14}$$

The transmission component uses internal logic to shift gears, whereas the differential has a fixed gear ratio. The motor and engine components use two-dimensional interpolation to reference efficiency from a map using Equation 15.

$$P_b = \tau_f \omega_f \eta\left(\tau_f, \omega_f\right)^{-\text{sign}\left(\tau_f\right)} \tag{15}$$

Finally, battery and fuel tank models integrate the required power to track remaining energy using Equations 16 and 17.

$$P_{\text{batt}} = P_{b,\,\text{motor}} \tag{16}$$

$$E_{\text{batt}} = E_{\text{batt}} - P_{\text{batt}}\Delta t \tag{17}$$

The Forward Step. Each component has limitations such as maximum torque, speed, or power. In cases in which these limits are exceeded, torque or force will be reduced. For example, if the motor exceeds its maximum speed, its torque output falls to zero, and zero power is demanded from the battery. If the motor exceeds its maximum

torque, its torque output is reset to the maximum available torque. Additionally, the energy storage component may exhaust its energy, meaning that no power can be supplied to the motor, and the motor cannot supply torque to the other components. To propagate component limitations through the drivetrain, each component takes a forward step to check that the component behind it was able to meet the demands of the drive cycle. This process starts with the engine or motor models verifying that energy is available from the energy storage system and adjusting output torque to reflect any reduction in power output. These steps are shown in Equations 18 and 19.

$$P_{b,\text{motor}} = P_{\text{batt}} \tag{18}$$

$$\tau_f = \frac{P_b}{\omega_f}\eta^{\text{sign}(P_b)} \tag{19}$$

Next, the information is propagated to the transmission and differential (Equations 20 and 21) followed by the wheel (Equations 22 and 23).

$$\tau_{b,\text{transmission}} = \tau_{f,\text{motor}} \tag{20}$$

$$\tau_f = \tau_b r_{\text{gear}} \tag{21}$$

$$\tau_{b,\text{wheel}} = \tau_{f,\text{differential}} \tag{22}$$

$$F_f = \frac{\tau_b}{r_{\text{tire}}} \tag{23}$$

Finally, the vehicle speed is recalculated in the chassis model shown in Equation 24.

$$v = \frac{F_{f,\text{wheel}} + \frac{vm}{\Delta t} - C_{rr}\text{mgcos}(\theta) - \text{mgsin}(\theta)}{\frac{m}{\Delta t} + \frac{1}{2}\rho C_d A v} \tag{24}$$

In the event that every component was able to supply the contribution demanded of it, the speed calculated at the end of the forward step will be equal to the logged speed. If not, the speed will be less than the logged speed. For scenarios in which the battery is unable to supply power, $P_{\text{batt}} = 0$, the forward step will propagate this information through the drivetrain until $F_{f,\text{wheel}}$, the force provided by the drivetrain, is 0, reducing Equations 24 to 25, which simulates a coast down.

$$v = \frac{\frac{vm}{\Delta t} - C_{rr}\text{mgcos}(\theta) - \text{mgsin}(\theta)}{\frac{m}{\Delta t} + \frac{1}{2}\rho C_d A v} \tag{25}$$

Results and Discussion

Vehicle mass plays an important role in understanding vehicle energy consumption for both BEBs and CDBs. Energy consumption under three different payloads (i.e., zero payloads, maximum payload, and time-varying payload) were investigated for both a BEB and CDB. The zero-payload scenario was modeled at a vehicle mass of 14,322 kg, and the max payload scenario was modeled at a mass of 19,799 kg, which is the curb weight and gross vehicle weight rating respectively of the Proterra E2 + electric bus. Although actual CDBs are generally lighter, both buses were modeled at the same weights for this study. The time-varying payload experienced weight variations for passenger loadings between 2 and 21 daily average passengers. Figure 2 shows the energy consumption per mile versus daily vehicle mass with zero payloads, time-varying payload, and max payload represented by the green triangles, blue circles, and red squares, respectively.

The dashed trend line in Figure 2 indicates a positive correlation between vehicle mass and energy consumption for both kinds of buses, thus confirming that vehicle mass plays an important role in understanding vehicle energy consumption regardless of drivetrain type. The buses use more energy as more passengers board, with a 34% average increase for the max payload CDB over the empty CDB compared with a 23% average increase for the max payload BEB over the empty BEB. In relation to sensitivity to added vehicle mass, the CDB increases at a rate of 0.63 Wh/(mi-kg), whereas the BEB increased energy consumption at a 0.05 Wh/(mi-kg) rate. It should be noted that the energy consumption of the CDB was calculated based on the energy content in the fuel consumed assuming 37.6 kWh/gal. The lower sensitivity of the energy consumption of the BEB as compared to the CDB can be attributed to the increase in drivetrain efficiency as well as the ability of the BEB to recapture energy through regenerative braking. With greater mass, the BEB both expends and recaptures more kinetic energy, whereas the CDB only uses more energy. However, this increased regeneration is not guaranteed as braking is controlled by the operator, and there is a maximum energy recapture rate of an electric vehicle. Therefore, the vehicle's control system and the operator may benefit from knowing the vehicle mass allowing them to maximize regenerative braking.

Driving aggressiveness can exacerbate the effect of increased payload. Kinetic intensity (KI), the ratio of characteristic acceleration ($\tilde{a}$) to aerodynamic velocity (v^2_{aero}), is a metric used to describe the aggressiveness of drive cycles and is often used to estimate the benefits of hybridizing or electrifying an existing drivetrain (Equation 26) (*16*).

$$KI = \frac{\tilde{a}}{v^2_{\text{aero}}} \cong \frac{\sum_{j=1}^{N-1}\text{positive}\left(\frac{1}{2}\cdot\left(v^2_{j+1} - v^2_j\right) + g\cdot\left(h_{j+1} - h_j\right)\right)}{\sum_{j=1}^{N-1}\overline{v^3_{j,j+1}}\cdot\Delta t_{j,j+1}} \tag{26}$$

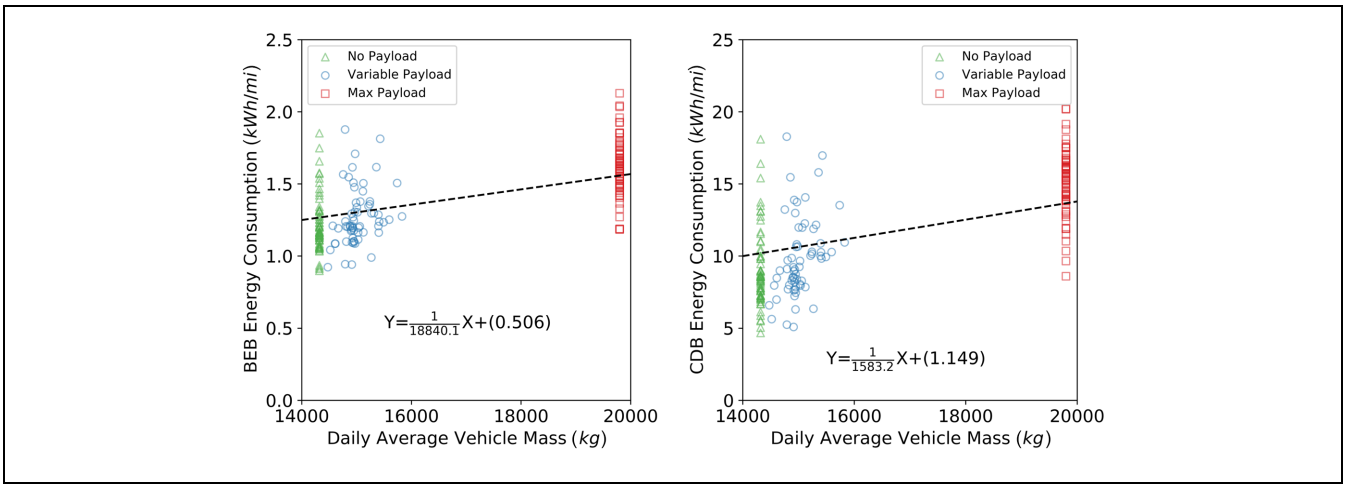

Figure 2. Energy consumption correlation with bus mass between empty and full payloads.

Figure 3. Daily average KI values by vocation from the FleetDNA database (n = 700).

Higher KI indicates a trip with frequent acceleration/deceleration and slower speeds. Lower KI is evidence of less frequent starts and stops as well as higher speeds. If the goal is to improve fuel economy, vehicles with high KI benefit most from regenerative braking, whereas vehicles with low KI are more conducive to aerodynamic devices like skirts or fairings. KI only characterizes driving behavior and does not account for the mass or drag coefficient of the vehicle. Figure 3 provides a violin plot of log-scale KI for five common vocations throughout 101 vehicle-days of data. This plot was generated using data from the National Renewable Energy Laboratory's FleetDNA vehicle database. The white dot and black box for each vocation represent the median and interquartile ranges respectively, and the black lines are the 95% confidence intervals like in a box plot. In addition, the outer violin shape is generated for each location based on the kernel density of the data providing an understanding of where the majority of the vehicles lie. Transit buses have a relatively high KI compared with other common vocations indicating that the transit buses drive cycle may be a good candidate for regenerative braking and that vehicle mass will have a large effect on energy consumption.

To test this hypothesis, we compared the increase in energy consumption a loaded bus would have over the unloaded bus versus KI for both the CDB and BEB. The KI of the measured routes varied from 0.27 to 4.69 mi^{-1}. Both time-varying payload (blue circles) and max payload (red squares) were compared with no payload, and the relative increase is shown by percentage in Figure 4. As expected, energy used relative to an unloaded bus increases with increasing KI for all cases. Additionally, the CDB shows a larger increase for higher KIs than that of the BEB, confirming the benefit from regenerative braking; that is, with frequent stops/starts and lower speeds, more energy is recovered by the BEB.

As KI reaches 4 mi^{-1}, Figure 4 shows the BEB has a 45% increase in energy consumption as compared to a 20% increase for a KI of 0.5 mi^{-1} in the case of max payload. The time-varying payload case only shows a 4% increase in energy consumption for a KI of 0.5 mi^{-1} and an 8% increase for a KI of 4 mi^{-1}. Similarly, the CDB has about a 100% increase in energy use for the max payload for a KI of 4 mi^{-1} compared with a 45% increase for a KI of 0.5 mi^{-1} in the case of max payload. The time-varying payload case shows a 6% increase in energy consumption for a KI of 0.5 mi^{-1} and a 15% increase for a KI of 4 mi^{-1}. This means that for the 38% increase in vehicle mass between the unloaded and max payload case, there is an even greater increase in energy consumption. Moreover, a few instances for the CDB had a 115% increase in energy consumption, three times that of the weight increase. The variable payload case was less affected by increasing KI; however, for both the BEB and CDB there was a positive correlation between

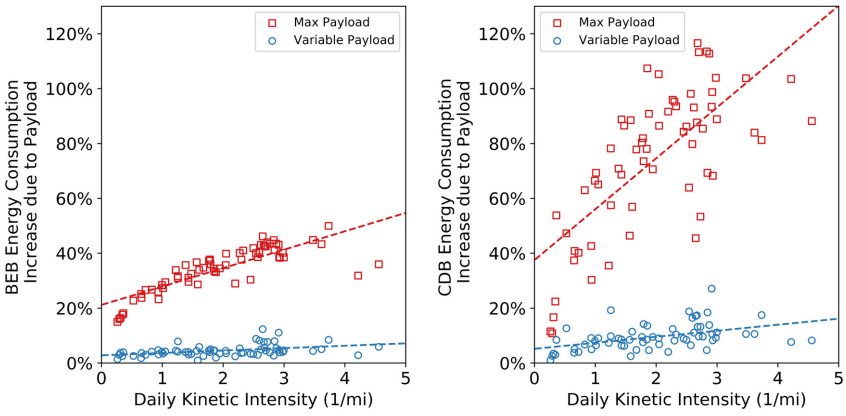

Figure 4. Energy consumption increase with trip KI owing to payload for BEB and CDB.

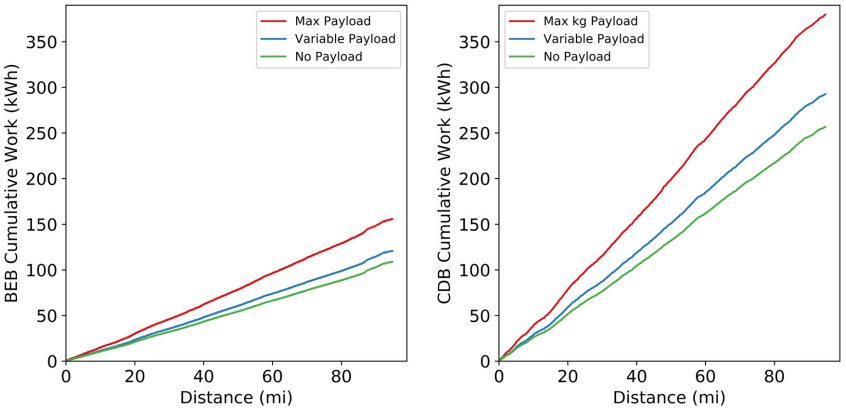

Figure 5. Single day payload comparison of cumulative tractive work for the BEB and CDB.

energy consumption and KI. It is possible that other routes or cities with higher transit utilization would have passenger payloads closer to that of the max payload case.

This high sensitivity of energy consumption to vehicle mass at high KI shows the value of knowing real-time mass estimation. For instance, if a transit agency is trying to determine optimal route selection or battery size for BEBs, knowing the passenger payload would help inform these decisions by allowing them to properly estimate the energy use throughout the day. Figure 5 provides a comparison of cumulative work versus distance for the BEB and CDB during one selected day of operation. The red, blue, and green lines represent max payload, time-varying payload, and no payload, respectively. Both the CDB and the BEB show higher work rates as the vehicle gets heavier. For the example day shown in Figure 5, the CDB expends a total of 380 kWh, 293 kWh, and 257 kWh for the max payload, time-varying payload, and no payload cases respectively, and the BEB uses a total of 156 kWh, 121 kWh, and 109 kWh respectively. The difference in total work between no payload and the max payload case for the CDB was 47.9%, whereas the difference for the BEB was only 43.1% indicating the BEB is less sensitive to mass fluctuations than the CDB. Although most CDBs have enough fuel capacity to cover this difference in work, a BEB may be limited depending on the size of the battery, thus limiting the overall driving range of the vehicle. Additionally, Figure 5 shows that cumulative work increases at a higher rate for the CDB compared with the BEB, which is again attributed to the lack of regenerative braking.

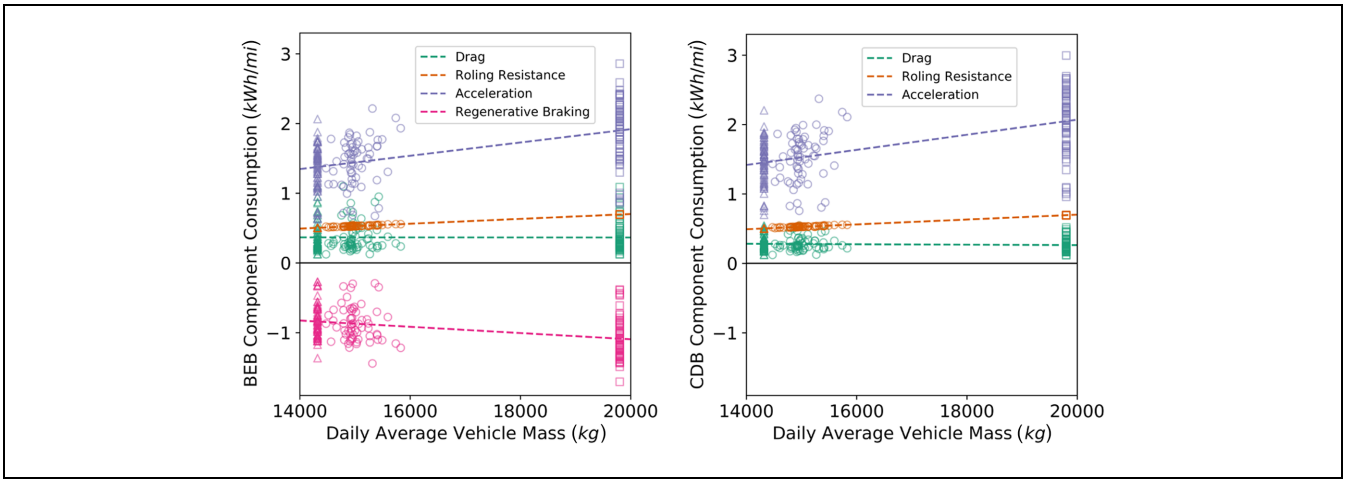

Figure 6. Energy consumption of drag, rolling resistance, acceleration, and regenerative braking versus trip average vehicle mass for BEB and CDB.

The influence of a vehicle's mass on its energy consumption can be explained by examining the energy consumption from each component of the road load equation, shown in Figure 6. For both buses, as mass increases, the energy used to accelerate the vehicle increases proportionally along with the rolling resistance to a lesser extent, though the energy to overcome drag remains constant. However, as mentioned previously, vehicle mass has a smaller influence on the energy consumption of the BEB, which can be explained by its ability to recapture energy through regenerative braking. As the mass increased on the BEB, the vehicle's total kinetic energy increased, meaning there was more energy to recapture during braking events. Figure 6 confirms this by showing that while total energy consumption increases proportionally to vehicle mass, the energy regained from regenerative braking increases as well. The results agree with Yu's study that the impacts of passenger load on fuel consumption are directly influenced by accelerations (*16*).

Conclusion

This research applied a novel mass detection technique to determine the impact of time-varying mass on bus energy consumption. Real-world driving data and real-time vehicle mass-estimates were combined with a drive-train model to evaluate the impact of vehicle payload on energy consumption. The results in this paper show that as the vehicle mass increased, energy consumption for both the CDB and BEB increased proportionally. The CDB had a greater sensitivity to increases in vehicle payload over the BEB, which can be explained by the BEB's ability to recapture energy through regenerative braking. Further, the increase in energy consumption from payload was a result of the extra work required to accelerate the vehicle and, to a lesser extent, to overcome rolling resistance. Despite this increased impact on CDBs, most CDBs had enough fuel to account for any increases in energy consumption such that their ability to perform their duty was not affected. However, increases in vehicle payload may limit the driving range of a BEB and affect its ability to perform the route if the battery is not sized to consider the range of passenger load. Driving aggressiveness as measured by KI was also shown to have a larger impact on energy consumption at higher KIs with the CDB showing the greatest sensitivity for a KI of $4\,\mathrm{mi}^{-1}$ resulting in a 115% increase in energy consumption for the max payload case, and only a 15% increase for the variable payload. Despite the relatively low increase for the variable payload case, it is possible that other routes or cities with higher transit utilization would have passenger payloads closer to that of the max payload case.

Only 65 days of data and three buses were used in this study; therefore, further research with a larger vehicle dataset including more buses and routes with higher utilization is planned to fully investigate potential transit bus driving scenarios. Future work will also involve analyzing real-world energy efficiency under different payloads for both in-use BEBs and CDBs to validate the modeled results reported in this study. Outcomes of these future studies may include identifying specific routes that will realize the most savings from electrification by properly categorizing energy requirements resulting from aggressive driving and passenger payload. Results could also be used to plan more energy-efficient routes and to schedule on-route fast charging of BEBs.

Acknowledgments

Funding for this work came from the Transit IDEA Program, as part of the Transportation Research Board (project number:

163615-0399). We acknowledge Twin Cities Metro Transit for providing access to the transit buses used in this study, specifically David Haas for his technical contributions to this work.

Author Contributions

The authors confirm contribution to the paper as follows: study conception and design: WN, LL, AK; data collection: LL, AS; analysis and interpretation of results: AK, LL, WN, EM; draft manuscript preparation: WN, LL, AK, EM. All authors reviewed the results and approved the final version of the manuscript.

References

1. Nylund, N. O., K. Erkkilä, and T. Hartikka. *Fuel Consumption and Exhaust Emissions of Urban Buses*. VTT Tiedotteita Research Notes, 2373, 2007.
2. Eudy, L., M. B. Post, and M. A. Jeffers. *Zero Emission Bay Area (ZEBA) Fuel Cell Bus Demonstration Results: Sixth Report*. Publication NREL/TP–5400-68413. National Renewable Energy Laboratory, Colo., 2017.
3. Lajunen, A. Energy Consumption and Cost-Benefit Analysis of Hybrid and Electric City Buses. *Transportation Research Part C: Emerging Technologies*, Vol. 38, 2014, pp. 1–15.
4. Hwang, J., X. Li, and W. Northrop. *Exploration of Dual Fuel Diesel Engine Operation with On-Board Fuel Reforming*. SAE Technical Paper 2017-01-0757. Society of Automotive Engineers, Detroit, 2017.
5. Vollaro, R. D. L., L. Evangelisti, G. Battista, P. Gori, C. Guattari, and A. Fanchiotti. Bus for Urban Public Transport: Energy Performance Optimization. *Energy Procedia*, Vol. 45, 2014, pp. 731–738.
6. Lammert, M. P., A. Duran, J. Diez, K. Burton, and A. Nicholson. Effect of Platooning on Fuel Consumption of Class 8 Vehicles Over a Range of Speeds, Following Distances, and Mass. *SAE International Journal of Commercial Vehicles*, Vol. 7, 2014, pp. 626–639.
7. Alam, A., and M. Hatzopoulou. Investigating the Isolated and Combined Effects of Congestion, Roadway Grade, Passenger Load, and Alternative Fuels on Transit Bus Emissions. *Transportation Research Part D: Transport and Environment*, Vol. 29, 2014, pp. 12–21.
8. Zhang, S., Y. Wu, H. Liu, R. Huang, L. Yang, Z. Li, L. Fu, and J. Hao. Real-World Fuel Consumption and CO_2 Emissions of Urban Public Buses in Beijing. *Applied Energy*, Vol. 113, 2014, pp. 1645–1655.
9. Tolouei, R., and H. Titheridge. Vehicle Mass as a Determinant of Fuel Consumption and Secondary Safety Performance. *Transportation Research Part D: Transport and Environment*, Vol. 14, 2009, pp. 385–399.
10. Yu, Q., T. Li, and H. Li. Improving Urban Bus Emission and Fuel Consumption Modeling by Incorporating Passenger Load Factor for Real World Driving. *Applied Energy*, Vol. 161, 2016, pp. 101–111.
11. Tong, H. Y., W. T. Hung, and C. S. Cheung. On-Road Motor Vehicle Emissions and Fuel Consumption in Urban Driving Conditions. *Journal of the Air & Waste Management Association*, Vol. 50, No. 4, 2000, pp. 543–554.
12. Wang, A., Y. Ge, J. Tan, M. Fu, A. N. Shah, Y. Ding, H. Zhao, and B. Liang. On-Road Pollutant Emission and Fuel Consumption Characteristics of Buses in Beijing. *Journal of Environmental Sciences*, Vol. 23, 2011, pp. 419–426.
13. McDowell, M. A., C. D. Fryar, C. L. Ogden, and K. M. Flegal. *Anthropometric Reference Data for Children and Adults: United States, 2003–2006*. National Health Statistics Reports No. 10. National Center for Health Statistics, Hyattsville, Md., 2008, pp. 1–45.
14. Geller, B., and T. Bradley. Quantifying Uncertainty in Vehicle Simulation Studies. *SAE International Journal of Passenger Cars-Mechanical Systems*, Vol. 5, 2012, pp. 381–392.
15. Brooker, A., J. Gonder, L. Wang, E. Wood, S. Lopp, and L. Ramroth. *FASTSim: A Model to Estimate Vehicle Efficiency, Cost and Performance*. SAE Technical Paper 2015-01-0973. Society of Automotive Engineers, Detroit, 2015.
16. O'Keefe, M. P., A. Simpson, K. J. Kelly, and D. S. Pedersen. *Duty Cycle Characterization and Evaluation towards Heavy Hybrid Vehicle Applications*. SAE Technical Paper 2007-01-0302. Society of Automotive Engineers, Detroit, 2007.

The Standing Committee on Bus Transit Systems (AP050) peer-reviewed this paper (19-03047).